Metabolic Flux Distributions in *Corynebacterium glutamicum* During Growth and Lysine Overproduction

Joseph J. Vallino* and Gregory Stephanopoulos†
Chemical Engineering Department, Massachusetts Institute of Technology, Cambridge, Massachusetts 02139

Received May 1, 1992/Accepted September 28, 1992

The two main contributions of this article are the solidification of *Corynebacterium glutamicum* biochemistry guided by bioreaction network analysis, and the determination of basal metabolic flux distributions during growth and lysine synthesis. Employed methodology makes use of stoichiometrically based mass balances to determine flux distributions in the *C. glutamicum* metabolic network. Presented are a brief description of the methodology, a thorough literature review of glutamic acid bacteria biochemistry, and specific results obtained through a combination of fermentation studies and analysis-directed intracellular assays. The latter include the findings of the lack of activity of glyoxylate shunt, and that phosphoenolpyruvate carboxylase (PPC) is the only anaplerotic reaction expressed in *C. glutamicum* cultivated on glucose minimal media. Network simplifications afforded by the above findings facilitated the determination of metabolic flux distributions under a variety of culture conditions and led to the following conclusions. Both the pentose phosphate pathway and PPC support significant fluxes during growth and lysine overproduction, and that flux partitioning at the glucose-6-phosphate branch point does not appear to limit lysine synthesis. © 1993 John Wiley & Sons, Inc.
Key words: flux analysis • metabolic engineering • *Corynebacterium glutamicum* • lysine

INTRODUCTION

Standard practice for strain improvement of industrial microorganisms involves exposing a product-producing strain to a mutagen, then selecting for those mutants which exhibit a desired phenotype and testing the derived strains for improved productivity or yield.[13] In this type of procedure, the alterations of the parent strain's genome cannot be easily resolved due to the nonspecific effects of the mutagens employed, so that the genetic modifications that lead to improved strains may go undetermined or be incorrectly attributed to the phenotype selected for. Although genetic engineering techniques[3] can be used to remove the ambiguities associated with nonspecific mutagens, the enzymes that should be modified to increase product yield or productivity are often unknown, so that the extra effort required by genetic engineering techniques may not be rewarded with an equivalent improvement in strain enhancement. This is especially true when strain improvement requires modifications of the primary metabolic enzymes which are not obviously associated with the product of interest. Consequently, mutation-selection is still often a faster approach for strain improvement. As case in point involves lysine production by glutamic acid bacteria.[25]

It is well established that strains of glutamic acid bacteria (typically *Corynebacterium glutamicum, Brevibacterium flavum,* and *Brevibacterium lactofermentum*) can be obtained that produce significant amounts of lysine (ca. 30% molar yield) by selecting for mutants that exhibit *S*-(2-aminoethyl) L-cysteine resistance (AEC, a lysine antimetabolite), which dramatically enhances selecting strains with feedback-resistant aspartate kinase.[11,74] Deregulation of lysine synthesis, however, does not result in the maximum yield (75% molar),[68] so that mutation-selection techniques have focused on modifying enzymes of the primary metabolism, such as citrate synthase,[59] the pyruvate dehydrogenase complex[44,75] (PDC), pyruvate kinase[61,65] (PK), and phosphoenolpyruvate carboxylase[88] (PPC). Although these modifications have resulted in a strain that produces lysine at a 55% molar yield,[62] it is not known in what respect(s) this strain differs from the original parent strain. Indeed, genetic engineering approaches have yet to make significant improvements in lysine yield[11,32,50] due to the inability of deciphering the results obtained from mutation-selection.

Although techniques such as metabolic control theory,[15] biochemical systems theory,[67] whole-cell kinetic models,[23] stable[21] and radio[6] isotope tracers, and linear analysis[45] have been applied to metabolic networks, significant information regarding potential metabolic bottlenecks can be obtained from mass balance techniques.[36,38,46,76,80,81,83] The latter are readily applied and do not require information regarding enzyme kinetics. In this study we utilized these mass balance techniques in conjunction with intracellular assays to solidify the biochemistry of *C. glutamicum* ATCC 21253, and to examine metabolic flux distributions during growth and lysine overproduction to establish the basal case for subsequent perturbation studies.

MATERIALS AND METHODS

Microorganism and Medium

The organism *C. glutamicum* ATCC 21253, obtained from the American Type Culture Collection (ATCC, Rockville,

* Present address: Scripps Institution of Oceanography, University of California, San Diego, La Jolla, CA 92093–0202.
† To whom all correspondence should be addressed.

CCC 0006-3592/93/060633-014

MD), was used in all experiments described below. *C. glutamicum* ATCC 21253 requires biotin, homoserine (or threonine plus methionine), and leucine for growth and produces lysine under threonine limitation. Stock cultures of this organism were stored at −70°C in LB5G medium (5 g/L glucose, 5 g/L yeast extract, 10 g/L tryptone, 5 g/L NaCl) supplemented with 10% (v/v) glycerol. Working cultures of this organism were maintained at 4°C on LB5G plates (1.8% agar) and transferred at 1-month intervals.

Cultures for fermentation or intracellular assays were started from a seed culture consisting of 50 mL of LB5G medium in a 250-mL baffled Erlenmeyer flask (Belco, Vineland, NJ), and inoculated with a small colony of the working culture that had been growing overnight on a LB5G plate at 30°C. The seed culture, grown at 30°C under agitation (ca. 250 rpm) for 10 h, was used to inoculate 1 L of preculture medium (PMB), which was cultivated in a 4-L baffled Erlenmeyer flask at 30°C on a rotary shaker at 150 rpm. The PMB medium[84] was autoclaved at 121°C for 20 min in three separate parts: (A) 20 g glucose, 1.14 g citrate · Na_3 · $2H_2O$, 55 mg $CaCl_2$, 200 mg $MgSO_4$ · $7H_2O$, 20 mg $FeSO_4$ · $7H_2O$, 1 g NaCl, 10 mL 100× mineral salts, diluted to 800 mL with distilled water and adjusted to pH 5.0 with HCl; (B) 8 g K_2HPO_4, 1 g KH_2PO_4, 150 mg threonine, 100 mg leucine, 40 mg methionine, 0.5 mg biotin, 1 mg thiamine · HCl, diluted to 100 mL; (C) 5 g $(NH_4)_2SO_4$ in 100 mL distilled water; 100× mineral salts: 200 mg/L $FeCl_3$ · $6H_2O$, 200 mg/L $MnSO_4$ · H_2O, 50 mg/L $ZnSO_4$ · $7H_2O$, 20 mg/L $CuCl_2$ · $2H_2O$, 20 mg/L $Na_2B_4O_7$ · $10H_2O$, 10 mg/L $(NH_4)_6Mo_7O_{24}$ · $4H_2O$, adjusted to pH 1.5 with HCl. After 10 h of incubation, the preculture attained a dry cell weight (DCW) of approximately 3 g/L (OD_{660nm} of 11; DCW = 0.28 * OD) and was either harvested for intracellular assays or used as an inoculum for the fermentor. Yeast extract, tryptone, and agar were obtained from Difco Laboratories (Detroit, MI); organic chemicals were from Sigma Chemical Co. (St. Louis, MO) except where noted, and salts were from Mallinckrodt, Inc. (Paris, KY).

Enzyme Assays

The preculture was cooled on ice to 4°C and centrifuged at 7000*g* and 4°C (J2-21 centrifuge, Beckman, Palo Alto, CA) for 5 min. The pellet was washed twice with cold extract buffer (100 m*M* tris · HCl, pH 7.5; 100 m*M* KCl; 10 m*M* Mg Cl_2) and resuspended to a final volume of 15 mL. Biomass concentration in the washed-cell concentrate was approximately 30 to 60 g DCW/L.

Cell homogenization was accomplished by ballistic disintegration with a MSK cell homogenizer (B. Braun Melsungen AG, Germany). A chilled 50-mL glass shaking bottle was used, to which 40.0 g of 0.10 to 0.11-mm glass beads (B. Braun) and 15 mL of the cell concentrate were added. The cell suspension was homogenized at 4000 rpm for 2 min and maintained at approximately 4°C by periodically sparging the vessel with liquid CO_2. The cell homogenate was separated from the glass beads by passing the suspension through glass wool, then centrifuged at 48,000*g* and 4°C for 45 min.

Biuret reagent (Sigma) was used to determine total protein, where bovine serum albumin (Serva, Westbury, NY) was used as the standard. Isocitrate lyase (ICLY) activity was measured according to Darton and Gunsalus.[14] Oxaloacetate decarboxylase (OaADC) activity was determined by measuring formation of pyruvate and removal of oxaloacetate (OaA).[34,73] Activity of phosphoenolpyruvate (PEP) synthetase (PPS) was determined by the ATP-dependent removal of pyruvate.[9] Phosphoenolpyruvate carboxylase and pyruvate carboxylase (PC) activities were independently measured by coupling OaA production with malate dehydrogenase and monitoring the disappearance of NADH.[73] Malic enzyme activity was measured by monitoring changes in NADPH concentration.[20] The activity of the PDC was measured by following acetyl phosphate formation.[47] Glucose-6-phosphate (Glc6P) isomerase (GPI) assay was run in reverse where Glc6P formation was measured by Glc6P dehydrogenase.[37] Activity of isocitrate dehydrogenase (ICDH) was measured by following changes in NADPH concentration.[16] All assays were conducted at 30°C.

Fermentation

Batch fermentations were conducted in a 15-L MBR Laboratory Bioreactor (MBR Bio Reactor AG, Wetzikon, Switzerland) with a 10-L working volume at 30°C. Aeration was controlled at 1 vvm (10 L/min) by a Brooks 5850E mass flow controller (Brooks Prod., Gloucester, MA). Dissolved oxygen was monitored by an Ingold oxygen electrode (Ingold Electronics, Inc., Wilmington, MA) and was maintained above 10% saturation by manually adjusting impeller rpm. Culture pH was monitored by a Type 765 Ingold electrode and controlled at pH 7.0 by the addition of concentrated ammonium hydroxide (26% w/w NH_3). Weight of added ammonium hydroxide was monitored on-line by a digital balance (Ohaus Scale Corp., Florham Park, NJ).

To determined oxygen uptake rate (OUR) and carbon dioxide evolution rate (CER), the composition of fermentor feed- and off-gases were measured by a Dycor quadruple mass spectrometer (Ametex, Thermox Instruments Division, Pittsburgh, PA) as described by Coppella and Dhurjati.[10] Fermentor load cells were employed to determined culture volume used in OUR and CER calculations. All on-line variables were interfaced to a WYSE PC via a DT2801 Data Translation (Marlboro, MA) data-acquisition board and displayed graphically.[10,27]

The fermentation medium (FM4) was prepared in two parts: (A) 1500 g glucose (J. T. Baker, Inc., Jackson, TN), 10 g citric acid, 6 g $MgSO_4$ · $7H_2O$, 500 mg $FeSO_4$ · $7H_2O$, 20 g NaCl, 1 g $CaCl_2$, 200 mL 100× mineral salts, 10 mL poly(propylene glycol) (2000 av. MW, Polysciences, Inc., Warrington, PA), diluted to 7 L

with distilled water and adjusted to pH 4; (B) 40 g K_2HPO_4, 20 g KH_2PO_4, 7.33 g threonine, 15 g leucine, 6 g methionine, 10 mg biotin, 20 mg thiamine · HCl, 400 g $(NH_4)_2SO_4$, diluted to 2 L with distilled water. Part (A) of the FM4 medium was sterilized in the fermentor at 121°C for 40 min; part (B) was autoclaved separately for 30 min and aseptically added to the fermentor after cooling to room temperature. The fermentor was inoculated with 1 L of preculture and sampled periodically as needed.

Sample Analysis

Dry cell weight was determined by centrifuging 20-mL samples at 5000*g* for 5 min, washing the cell pellet twice with water, and drying it for 24 h at 80°C. The C, H, N, and O elemental composition of *C. glutamicum* during the fermentation was measured by MultiChem Laboratories (Lowell, MA) after the cell pellet had been lyophilized. Glucose, trehalose, acetate, and lactate were measured on a Waters (Bedford, MA) HPLC equipped with a Biorad (Rockville Centre, NY) Aminex HPX-87H reverse phase column. A Biorad Aminex HPX-87C reverse phase column was used to measure trehalose, alanine, valine, leucine, and threonine. Pyruvate,[34] ammonium,[5] lysine,[35] glutamate (Boehringer Mannheim kit No. 139 092, Indianapolis, IN) and sometimes glucose (Sigma kit No. 16-20) were measured enzymatically.

METABOLIC FLUX ESTIMATION

Theory

The carbon flow through the primary metabolic pathways of *C. glutamicum* was estimated from metabolite (i.e., mass) balances. The approach utilizes constraints imposed by the biochemistry, a pseudo-steady-state approximation for intracellular metabolites, and the measured accumulation rates of extracellular metabolites to generate flux distribution maps during the course of the fermentation. Although described in detail elsewhere,[81] a brief summary is given below.

The accumulation rate of a metabolite in a metabolic network is given by the summation of all reactions producing that metabolite minus the summation over all reactions consuming that metabolite:

$$r_i(t) = \sum_j \alpha_j x_j(t) - \sum_k \alpha_k x_k(t) \qquad (1)$$

where $x_j(t)$ is the rate or flux through reaction j, α_j is a stoichiometric coefficient, and $r_i(t)$ is the accumulation rate of metabolite i The set of equations formed from such balances constructed for each metabolite in the network is represented in matrix notation by

$$\mathbf{A}\mathbf{x}(t) = \mathbf{r}(t) \qquad (2)$$

where $\mathbf{A}$ is an $m \times n$ matrix of stoichiometric coefficients, $\mathbf{x}(t)$ an n-dimensional flux vector, and $\mathbf{r}(t)$ an m-dimensional metabolite accumulation rate vector. The weighted least squares solution[30] to Eq. (2), provided $m \geq n$ and $\mathbf{A}$ is of full rank, is

$$\hat{\mathbf{x}}(t) = (\mathbf{A}^T\boldsymbol{\Psi}^{-1}\mathbf{A})^{-1}\mathbf{A}^T\boldsymbol{\Psi}^{-1}\bar{\mathbf{r}}(t) \qquad (3)$$

where $\boldsymbol{\Psi}$ is the measurement noise covariance matrix associated with $\mathbf{r}$ and the superscripts $\hat{}$ and $\bar{}$ denote estimated and measured quantities, respectively.

The elements of $\mathbf{r}(t)$ are divided into two subvectors $\mathbf{r}_E(t)$ and $\mathbf{r}_I(t)$, which correspond to extracellular and intracellular metabolites, respectively. Accumulation rates for extracellular compounds [i.e., elements of $\mathbf{r}_E(t)$] are derived from the slope taken between two consecutive concentration data points, or directly from measurement, as is the case for OUR and CER. A pseudo-steady-state (PSS) approximation is used for intracellular metabolites, so that $\mathbf{r}_I(t)$ is set to $\mathbf{0}$. This approximation seems to be valid for most intracellular metabolites based on the following considerations.

To maintain a responsive metabolism, concentrations of intracellular metabolites in a reaction sequence usually range from 20% to 100% of their respective saturation constant,[2] which are typically less than 1 m*M* and almost never exceed 10 m*M*.[23] Because observed metabolic fluxes are typically greater than 1.0 mmol · g^{-1} DCW · h^{-1} (see Results section) and the volume of a *C. glutamicum* cell[18] is approximately 1 μL · mg^{-1} DCW, fluxes based on intracellular volume (not culture volume) are of the order of 1000 m*M* h^{-1}. Hence, an intracellular metabolite accumulation rate of 1 m*M* min^{-1}, which would significantly alter enzyme kinetics in less than 1 min, can be achieved with only a 6% difference between flows producing and consuming the metabolite. Consequently, metabolic control directives of the cell can be rapidly attained without significantly violating the PSS approximation.

The elements of $\mathbf{r}$ are given in the Appendix, where the observed extracellular metabolites are: acetate, alanine, ammonium, biomass, CO_2, glucose, lactate, lysine, oxygen, pyruvate, trehalose, and valine. Consistency analysis[81,86] was used to identify gross measurement errors, and the diagonal elements of $\boldsymbol{\Psi}$ were derived from the propagation of measurement variance for the extracellular components (variance for intracellular metabolites was effectively set to 0), where the measurement standard deviations used were: biomass, 5% (of mean); CER, 10%; glucose, 2%; lysine, 2%; ammonia, 5%; OUR, 10%; and ±2 mmol · 1^{-1} · h^{-1} for each of the six observed byproducts.

C. glutamicum Biochemistry

The metabolic network of *C. glutamicum* was constructed primarily from publications on glutamic acid bacteria (mostly from two closely related strains *Brevibacterium flavum* and *B. lactofermentum*[25]); however, some ambiguities were present that are clarified in this study, as discussed later in this section and elsewhere.[79]

Most or all of the enzymes of the Embden–Meyerhof–Parnas pathway,[41,56] the tricarboxylic acid cycle (TCA),[41,56,63] and the pentose phosphate pathway (PPP)[40,41,56,58,69] have been detected in *C. glutamicum* or related strains. Anaplerotic pathways[29] detected in glutamic acid bacteria include PPC,[57,73] PC,[73] malic enzyme,[56,57,73] and ICLY and malate synthase of the glyoxylate shunt.[42,43,56] Although some evidence exists that PEP carboxykinase and PEP carboxytransphosphorylase are present in *B. ammoniagenes,*[4] the findings are not well supported, so these reactions are not considered in this study. The transport of glucose and other mono- or disaccharides have been associated with three phosphotransferase systems.[60] Ammonium uptake is fulfilled predominately by glutamate dehydrogenase and glutamine synthetase, because aspartase exhibits little or no activity,[32] and alanine and leucine dehydrogenases have not been detected.[25]

Although the GS/GOGAT ammonium assimilation route[17] has been reported in glutamic acid bacteria,[82] it is not believed to operate at high ammonium ion concentrations found in the fermentation medium. Of the five amino acid transferases detected in *B. flavum,* only aspartase aminotransferase is included in the network as it accounts for 90% of the aminotransferase activity.[53] Three energy coupling sites are possible in the respiratory chain of *B. flavum;*[66] however, only two sites appear to translocate protons in *B. lactofermentum,*[24] so that the P/O ratio has been set at 2. The Entner–Doudoroff pathway has not been detected in glutamic acid bacteria cultured on glucose,[41,58] nor was it induced by gluconate.[79]

Although glutamic acid bacteria can grow on C_2, C_3, and C_4-metabolites, the gluconeogenesis pathway has not been well studied. However, fructose diphosphatase has been recently demonstrated in *B. flavum,*[60,70] and it is possible that PDC and PK are bypassed by OaADC and PPS, respectively, because the former has been detected at high activity[34,73] and we have detected the latter in *C. glutamicum* (Table I). The presence of either membrane-associated or membrane-free pyridine dinucleotide transhydrogenase has not been examined. However, because NADH, but not NADPH, is readily oxidized in cell-free extracts,[26] a transhydrogenase has not been included in the network. Lysine synthesis in glutamic acid bacteria occurs via the diaminopimelate (DAP) pathway,[48] because most of the enzymes of this pathway have been detected.[12]

Table I. Activity of anaplerotic reactions in cell-free extracts of *C. glutamicum* ATCC 21253 cultivated on glucose or acetate PMB medium.

	Activity (nmol/min/mg protein)		
Enzyme	Glucose	Acetate	Glucose + acetate
Isocitrate lyase	0	524	15
PEP synthetase	17	36	12
PEP carboxylase	270	—	—
Pyruvate carboxylase	0	—	—
Malic enzyme	1.3	—	—
OaA decarboxylase	275	—	—

In addition to the DAP pathway, an alternate pathway for the direct conversion of 2-amino-6-ketopimelate to meso-DAP has also been identified in glutamic acid bacteria,[33] and both pathways appear to support significant carbon flux.[51] Although the pathway for trehalose synthesis has not been investigated, the disaccharide has been detected by others,[85] so that the pathway utilized by yeast[8] is assumed to operate in *C. glutamicum.* Acetate synthesis occurs via phosphotransacetylase and acetate kinase.[52] Lactate is assumed synthesized via lactate dehydrogenase.

Evidence suggests that alanine[72] and valine[78] synthesis occur via the same pathways that have been identified in *Escherichia coli.*[31] Biomass synthesis was represented as a lump equation,[19,81] where metabolite yield coefficients were corrected to match the measured elemental composition of *C. glutamicum*: C, 47.6%; H, 6.46%; O, 31.0%; N, 11.8%; ash, 3.02%. To account for maintenance and futile cycles, a reaction was included to dissipate excess ATP.

Dependent Reactions

Once a proposed metabolic network is expressed mathematically, by Eq. (2), it is possible that the carbon flux through some (or all) reactions cannot be uniquely determined solely from measured metabolite accumulation rates, even if there are more equations than unknown fluxes (i.e., $m > n$), This occurs when the rank of $\mathbf{A}$, $R(\mathbf{A})$—the number of independent equations—is less than the number of unknown fluxes, n in which case $\mathbf{A}$ will be referred to as singular. The number of independent measurements that must be added, or the number of reactions that must be removed or constrained, to render $\mathbf{A}$ nonsingular is given by the dimension of the null space of $\mathbf{A}$, $N(\mathbf{A}) = n - R(\mathbf{A})$. However, as few as two reactions (if the network was constructed as described above) to as many as all the reactions in the network can be affected by constraining the flux of only one reaction.

Because each of the $N(\mathbf{A})$ vectors that span the null space of $\mathbf{A}$ defines a set of fluxes that cannot be uniquely determined, inspection of these vectors identifies the reactions that are affected by the introduction of additional constraints. Each of the $N(\mathbf{A})$ sets is referred to as a singular group and can be thought to contain one dependent reaction[1,77] or one degree of freedom. A singular group is eliminated by revolving its degree of freedom by specifying the value (typically zero) of one of the fluxes in the group. Intracellular assays are employed for this purpose. Singular groups that encompass large portions of the network must be carefully defined, because the choice of the imposed constraint can radically alter the flux distributions throughout the network and the location of principal nodes[68] as demonstrated below. However, if a reaction is observable (i.e., its flux can be uniquely determined), then the pathway can be included in the network even if it is not believed to be expressed in the organism. Two brief examples,

Table II. Isocitrate lyase activity (nmol · min^{-1} mg $protein^{-1}$) reported for various strains of glutamic acid bacteria cultured on either glucose or acetate.

Carbon source			
Glucose	Acetate	Organism	Reference
6[a]	[b]	*B. flavum* ATCC 14067	56
146	783	*B. flavum* ATCC 14067	54
50[c]	—	*B. flavum* ATCC 14067	42
112[d]	—	*B. flavum* ATCC 14067	42
0.8[c]	—	*C. glutamicum* ATCC 13032	42
69[d]	—	*C. glutamicum* ATCC 13032	42
—	770	*B. flavum* ATCC 14067	43
0	222	*B. flavum* 22LD	49

[a] Estimated from data.
[b] Not measured.
[c] Cultured under low biotin (2 μg/L).
[d] Cultured under high biotin (30 μg/L).

illustrating the identification of one local and one more extended singular group, are presented in the Appendix.

Several singular groups were identified following the initial construction of the *C. glutamicum* metabolic network. Fluxes in the two pathways that lead from meso-DAP to lysine[51] cannot be uniquely determined; however, this singular group is very local, so that the meso-DAP dehydrogenase pathway was removed from the network, which is equivalent to lumping the two pathways together. Several extended singular groups identified were associated with the anaplerotic pathways. Initial reports on the biochemistry of glutamic acid[55] indicated that α-ketoglutarate dehydrogenase was absent, so that a modified TCA cycle (also called the DCA cycle) that utilizes the glyoxylate shunt was proposed.[57] Although α-ketoglutarate dehydrogenase was later detected,[64] publications still implicated the DCA cycle as the major flux supporting pathway.[85,87] However, reported activity of ICLY varies considerably when glucose is used as the main carbon source (Table II), so that the degree of ICLY induction by glucose remains ambiguous, especially in *C. glutamicum*. Due to the extended nature of the singular group, identification of the dominate oxidative pathway (TCA or DCA) was quite important, because estimated flux distributions in the two networks, for the same $\mathbf{r}(t)$, are radically different (Fig. 1).

To remove the singularities (and ambiguities), intracellular activities of the anaplerotic reactions were examined for glucose and acetate cultures (Table I). The results indicate that the glyoxylate shunt is not induced by glucose nor by glucose plus acetate in *C. glutamicum* ATCC 21253, which implies that the TCA cycle is the main oxidative pathway. Neither PC nor the malic enzyme exhibit significant activity when *C. glutamicum* is cultured on the PMB medium, while PPC activity is quite high and appears to be the only anaplerotic reaction expressed. The activity of OaADC is also quite high and appears to be expressed constitutively (data not presented). However, PPC, PK, and OaADC compose a local singular group, so that OaADC was removed from the network, because growth could not occur on glucose if OaADC supported a significant flux.

The resulting metabolic network for *C. glutamicum*, given in the Appendix, was found to be nonsingular, well posed (condition number, as previously defined,[81] was 59) with 34 unknown fluxes (n) and 37 balance equations (m). Furthermore, detailed analysis[81] indicated that flux estimates would exhibit low sensitivity to measurement errors in $\mathbf{r}(t)$, because all elements of $\partial\hat{\mathbf{x}}(t)/\partial\bar{\mathbf{r}}(t)$ are of order one or less (sensitivity matrix not shown). Because the system was overdetermined by three equations, a consistency index[81,86] was calculated for each measurement vector to insure that mass balance constraints were satisfied to within error dictated by measurement uncertainty.

RESULTS AND DISCUSSION

Fermentation

Profiles of the measured extracellular on- and off-line variables for the lysine fermentation of *C. glutamicum* ATCC 21253, cultured on FM4 medium, are illustrated in Figure 2; and intracellular protein content and activity of a few selected enzymes measured during the fermentation are illustrated in Figure 3. These profiles were found to be very reproducible, because three similar fermentations produced almost identical results (data not shown). From observation, the fermentation can be broken down into four separate phases, as portrayed in Figure 2A, which illustrates the profiles of biomass, glucose, and lysine throughout the course of the fermentation.

Phase I of the fermentation is marked by balanced (exponential) growth with little to no byproduct accumulation (except CO_2). The duration of phase I, as well as the biomass concentration at the end of this phase, is governed by the initial supply of threonine, which, in concert

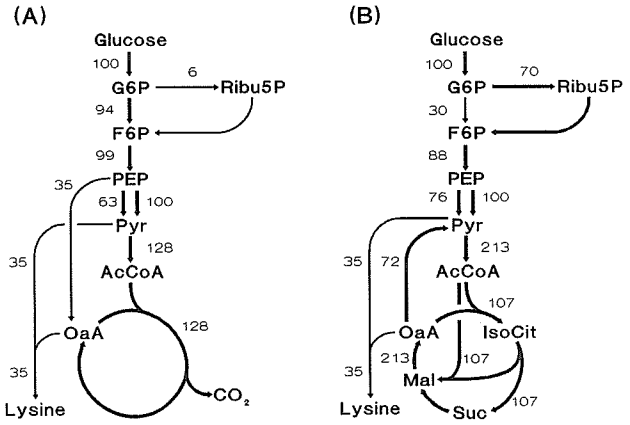

Figure 1. Theoretic flux distributions necessary to support a lysine molar yield of 35% in the *C. glutamicum* network (illustrated in condensed form) base on (A) the TCA or (B) the DCA oxidative cycle. The two fluxes between PEP and Pyr account for reactions catalyzed by PK (left) and the glucose: PEP phosphotransferase system (right). See Appendix for the complete set of reactions used in the analysis.

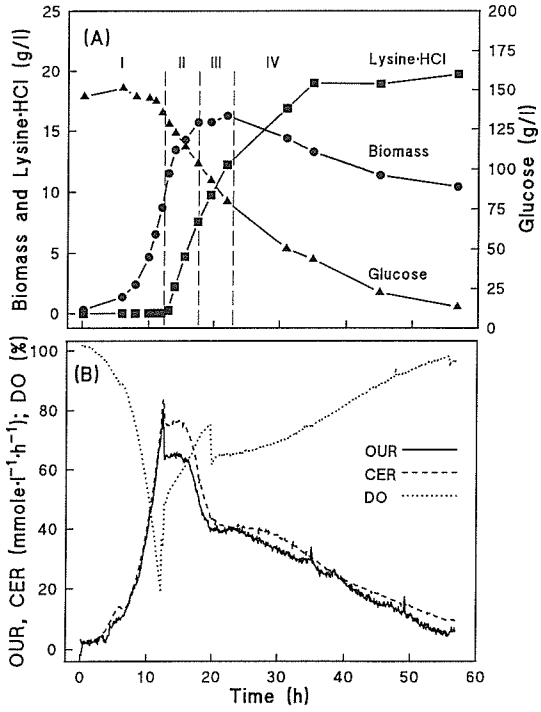

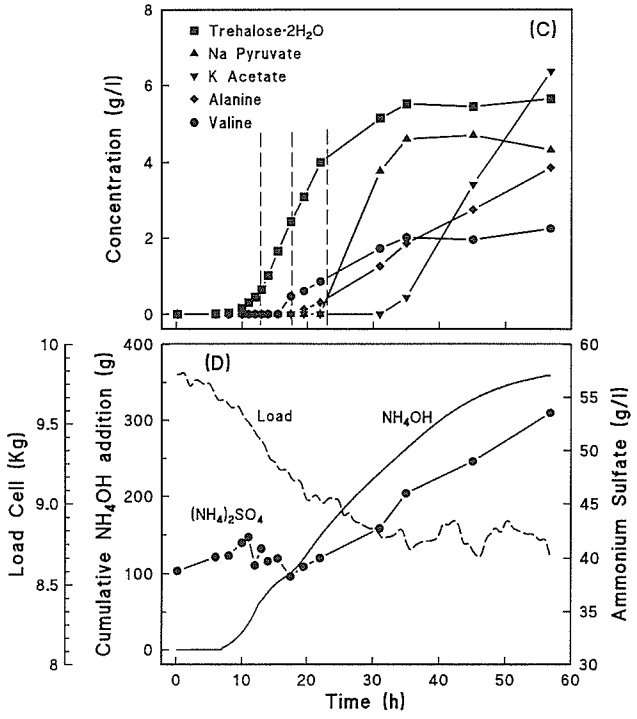

Figure 2. Lysine fermentation of *C. glutamicum* ATCC 21253 cultured on glucose FM4 medium. (A) glucose, biomass, and lysine · HCl profiles during the four phases of the culture. (B) Culture respiration: oxygen uptake rate (OUR), carbon dioxide evolution rate (CER), and dissolved oxygen (DO). (C) Accumulation of byproduct. (D) Available ammonium in broth, as $(NH_4)_2OH$; amount of ammonium hydroxide added to maintain culture at pH 7.0; and weight of fermentation broth.

with lysine, inhibits aspartate kinase[11] and prevents the overproduction of lysine.

Phase II of the fermentation commences at the exhaustion of supplied threonine, as evident by the break in

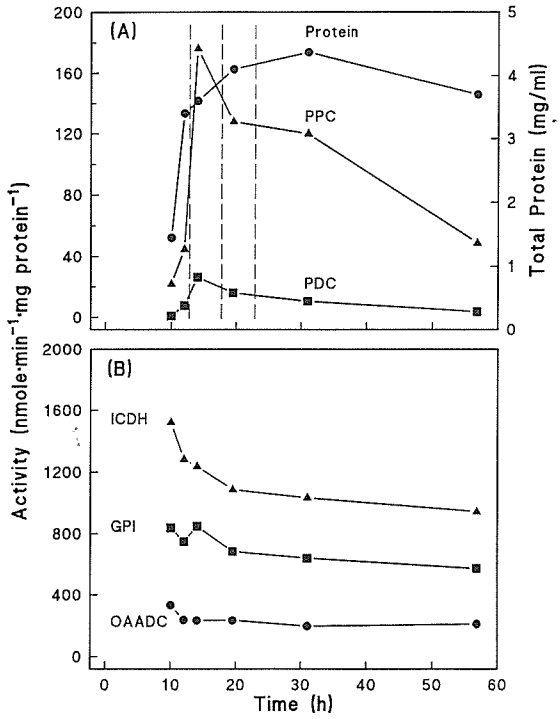

Figure 3. (A) Total soluble biomass-protein and intracellular activity of phosphoenolpyruvate carboxylase (PPC), pyruvate dehydrogenase complex (PDC); (B) isocitrate dehydrogenase (ICDH), glucose-6-phosphate isomerase (GPI), and oxaloacetate decarboxylase (OaADC) during the course of the lysine fermentation.

respiration (Fig. 2B), and is marked by high lysine and biomass production rates, constant respiration, and an elevated RQ of approximately 1.17, which is indicative of lysine overproduction.[27] The duration of phase II lasts approximately 4 to 5 hours, but can be extended by RQ controlled addition of threonine[27] or by culturing an AEC strain. The increase in biomass during this phase is probably due to either scavenging of threonine reserves (similar to that observed for trace nutrients[7]) or the accretion of cellular constituents,[71] including total protein (Fig. 3A). Changes in cellular morphology that accompany extracellular threonine depletion are quite complex and very important in lysine synthesis but have not been investigated.

Phase III of the culture commences as growth plateaus and is marked by high lysine production rates and decreasing respiration and RQ.

Phase IV of the culture basically represents the death phase as evident by the gradual reduction in lysine production, a decrease in biomass concentration, and a redirection of glucose to byproduct formation, such as pyruvate, acetate, alanine, and valine, as well as small amounts of a few unidentified metabolites, which may be associated with the loss of PDC activity (Fig. 3A) or TCA-related enzymes, such as the α-ketoglutarate dehydrogenase complex.[64] It is believed that the decrease in lysine synthesis in this phase results from the decay of primary enzymes, such as PPC (Fig. 3A), that can no longer be regenerated due to the lack of threonine and the loss of protein turnover

(if operational). Biomass samples analyzed in phases I, III, and IV did not vary significantly in elemental composition (data not shown).

The overall (integrated) lysine molar yield for the control fermentation was only 15%; however, the instantaneous molar lysine yield in each phase was phase I, 0%; phase II, 30%; phase III, 20%; phase IV, 10%. Although phase I of the culture could be effectively removed by employing an AEC strain of *C. glutamicum,* use of the latter strain would have prevented the study of the metabolic flux distributions associated with the transition to lysine overproduction. Similarly, fed-batch techniques[27] could be employed to remove phase IV; consequently, only phases II and III are of interest from a metabolic engineering perspective.

Metabolic Flux Estimation

Extracellular metabolite accumulation rates were calculated from Figure 2 during phase I at 11.5 h (sample points 5 and 6), phase II at 13.5 h (points 7 and 8) and 15.8 h (point 8 to 10), and phase III at 19.8 h (points 10 to 12). The consistency index,[81,86] h, calculated from accumulation rate vectors derived from data during phase IV exceeded the chi-square value of 6.25 for 3 degrees of freedom and a 90% confidence interval. Inconsistencies in data gathered during phase IV are believed to be due to the accumulation of compounds that could not be identified on the HPLC chromatograms; consequently, flux distributions during phase IV could not be estimated with confidence and are not presented. Metabolic flux distributions during phases I, II, and III, calculated from Eq. (3), are illustrated in Figures 4 to 7 and normalized with respect to glucose consumption rate (reaction 1) to facilitate comparison.

In regard to the overall network, the most dramatic metabolic transformation is observed between flux distributions in phase I and phase II of the fermentation (Figs. 4 and 5, respectively). This metabolic "perturbation" is induced by the sudden deregulation of lysine synthesis which causes a temporary flux redistribution in the primary metabolism from biomass toward lysine synthesis. It is during the early stages of phase II (Fig. 5) that the highest metabolic load is observed, because lysine and biomass production rates are both near their maximums during this period.

Subsequent flux distributions (Figs. 6 and 7) reflect a slow transition of the primary metabolism back to conditions similar to phase I, except that lysine production replaces biomass synthesis. In phase III, glucose is diverted toward trehalose and pyruvate-derived byproducts and the fluxes supported by glycolysis and the TCA cycle are diminished. General trends in individual reactions that can be discerned from the four "snap shots" of metabolic activity are summarized below.

Although the flux supported by the PPP, reaction 22, remains significant throughout all three phases of the fermentation, the transition from phase I to phase II (Figs. 4 and 5, respectively) is accompanied by an increase in flux through

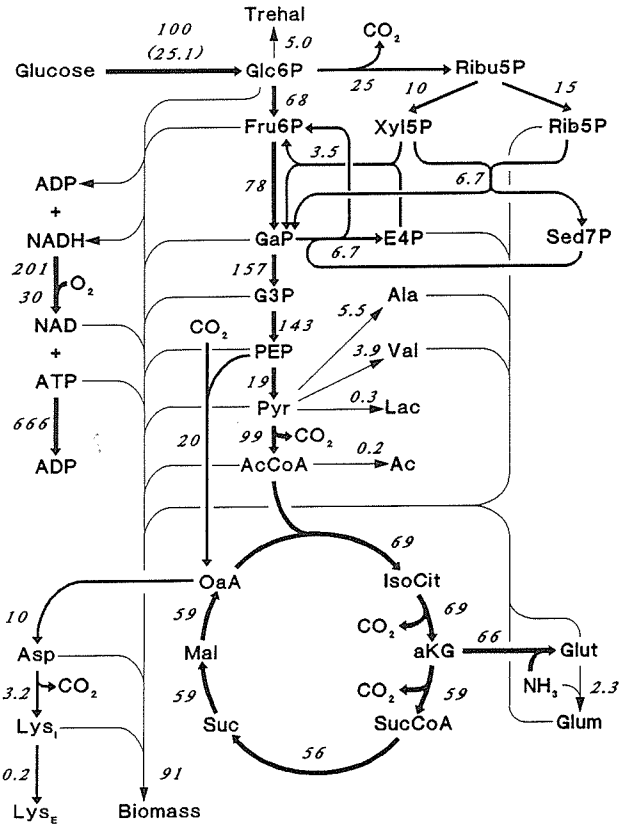

Figure 4. Flux distribution map for the lysine fermentation at 11.5 h (phase I). Flux estimates from measurements taken a 11.0 h and 12.0 h and normalized by glucose uptake rate (shown in parentheses: mmol · L^{-1} · h^{-1}). Consistency index, h, was 1.84.

this pathway to satisfy elevated NADPH requirements, but later subsides due to the decrease in biomass growth rate. The fraction of glucose catalyzed by PPC, reaction 9, is also quite significant for the four flux distributions analyzed and experiences a similar flux increase during the transition from phase I to phase II; likewise, PPC flux also returns to phase I conditions in phase III, which may be due to a reduction in PPC activity (Fig. 3A). The PPC reaction is extremely important, because it is the only anaplerotic reaction of the primary metabolism active when *C. glutamicum* is cultured on a minimal glucose medium. The flux distributions also demonstrate that PPC fixes large amounts of CO_2, which complicates quantitative analysis of metabolic tracer studies, as it is difficult to determine the extent of label enrichment in the CO_2 pool.

The fraction of glucose catabolized by the TCA cycle fluctuates around a mean and does not seem to exhibit any smooth trends. For instance, during phase I (Fig. 4), the TCA cycle flux is high but drops when lysine overproduction starts (Fig. 5) due to the diversion of metabolites to lysine synthesis at the PEP and Pyr branch points. In the later stages of phase II (Fig. 6) the TCA cycle flux returns to its former activity, but then drops again in phase III (Fig. 7) due to the diversion of glucose to byproducts. Intracellular activity of ICDH, as well as GPI and OaADC,

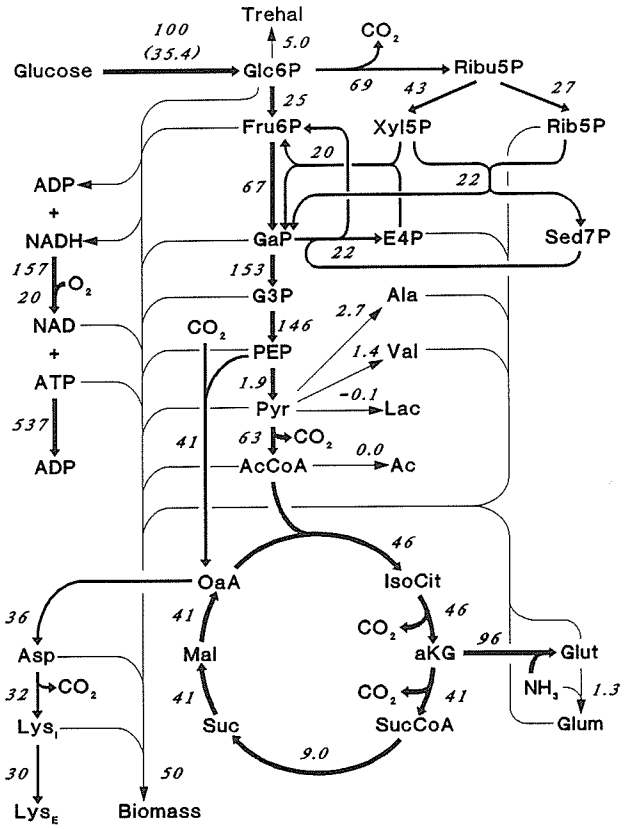

Figure 5. Flux distribution map for the lysine fermentation at 13.5 h (early phase II). Flux estimates from measurements taken at 13.0 h and 14.0 h and normalized by glucose uptake rate (shown in parentheses: mmol · L^{-1} · h^{-1}). Consistency index, h, was 0.25.

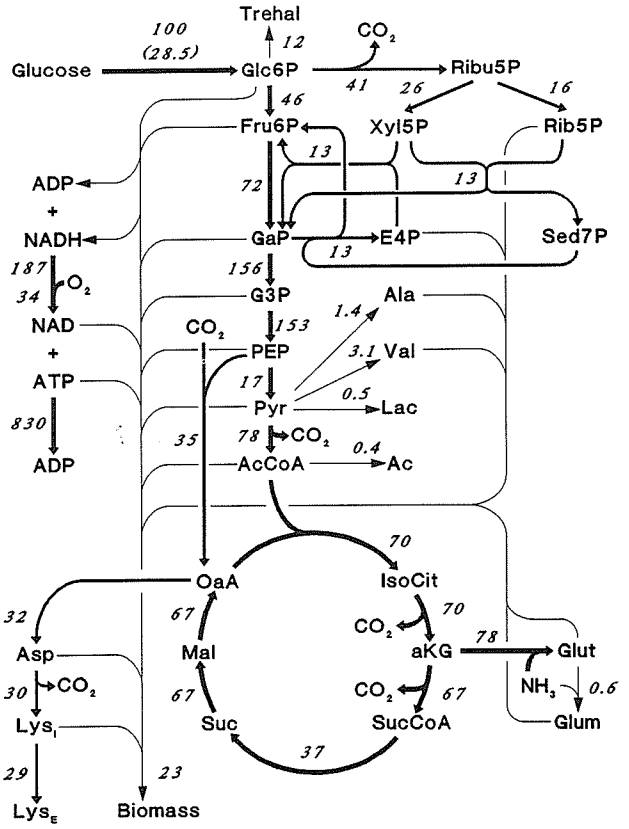

Figure 6. Flux distribution map for the lysine fermentation at 15.8 h (late phase II). Flux estimates from measurements taken at 14.0 h and 17.5 h and normalized by glucose uptake rate (shown in parentheses: mmol · L^{-1} · h^{-1}). Consistency index, h, was 0.40.

do not exhibit these trends (Fig. 3B). Not surprisingly, the excess ATP generated, reaction 34, fluctuates in step with the TCA cycle flux. Little information can be extracted from these fluctuations; however, maintenance requirements can be inferred as discussed below. Other reactions of interest include PK, reaction 7, which always exhibits a small flux due to the dominance of the PEP; glucose phosphotransferase system, reaction 1; and glutamate dehydrogenase, reaction 18, which always supports a large flux, because it is the primary reaction for the incorporation of free ammonia into amino acids.

Flux Verification

A first inspection of the fluxes in Figures 4 to 7 indicates that biochemical or thermodynamic constraints have not been violated (i.e., no negative flows in irreversible reactions). This almost trivial confirmation is important, for unacceptable flux distributions and constructed from consistent data, indicate errors or inconsistencies in the biochemistry network. For example, carbon fixation by the TCA cycle would signify that all functioning pathways have not been included in the network. For quantitative verification, the flux distributions were compared with radio (^{14}C) and stable (^{13}C) isotope tracer measurements cited in the literature for glutamic acid bacteria. In spite of questionable assumptions invoked to obtain quantitative flux distributions from metabolic tracers (for instance, flows to biomass and byproducts, and CO_2 fixing are often not accounted for), such measurement techniques are the only methods currently available for flux confirmation.

By far the most available and least controversial flux measurements involve the partitioning of glucose between the PPP and the Embden–Meyerhof–Parnas pathway (EMP). If it is assumed that the fraction of Fru6P recycled back into the PPP equals the fraction of glucose that enters the PPP,[58] as opposed to no recycle or total recycle of Fru6P, then the fraction of glucose consumed that enters the PPP (f_{PPP}) as a function of network fluxes is

$$f_{PPP} = \frac{\hat{x}_{22}}{\hat{x}_1 + \hat{x}_{26} + \hat{x}_{27}} \tag{4}$$

where the flows correspond to those listed in the Appendix. Listed in Table III is the calculated f_{PPP} from Eq. (4) based on the flux distributions illustrated in Figures 4 to 7. Table IV lists f_{PPP} reported from various literature sources.

Although the conditions under which f_{PPP} was measured vary markedly in Table IV, the results indicate that a substantial amount of glucose is catabolized through the PPP by glutamic acid bacteria. Furthermore, the measured values of f_{PPP} (Table IV) are consistent with the estimated values ob-

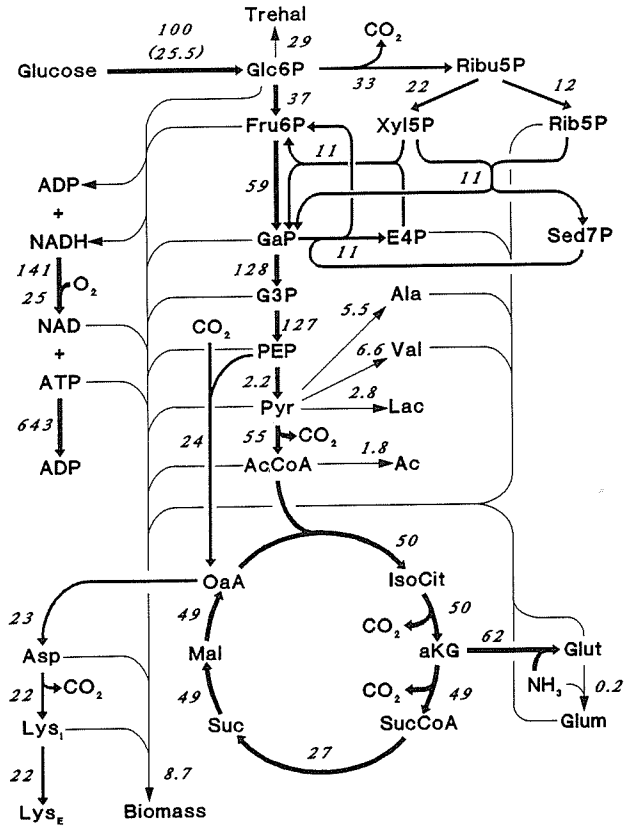

Figure 7. Flux distribution map for the lysine fermentation at 19.8 h (phase III). Flux estimates from measurements taken at 17.5 h and 22.0 h and normalized by glucose uptake rate (shown in parentheses: mmol · L^{-1} · h^{-1}). Consistency index, h, was 4.38.

Table III. Estimated fraction of glucose that enters the PPP [from Eq. (4) and Figures 4 to 7].

Phase: t_{ave} (h)	Figure	f_{PPP} (%)
I: 11.5	4	23
II: 13.5	5	49
II: 15.8	6	33
III: 19.8	7	27

tained from the flux distributions (Table III). Consequently, it is concluded that the estimated flux distributions between the PPP and EMP are in agreement with the state of the metabolism at the Glc6P branch point as represented by tracer studies. Although Yamaguchi et al.[87] and Inbar and Lapidot[21] investigated the flux distributions through the primary metabolism of *C. glutamicum* and *B. flavum*, respectively, using stable isotope tracers, their results are problematic, because they assumed the presence of the glyoxylate shunt, "single turn" operation of pathway cycles, and did not account for label enrichment due to CO_2 fixation. Nevetheless, their results indicate that the flux supported by PEP carboxylase, reaction 9, is significant (40% by their analysis), which is consistent with the results presented in Figures 4 to 7. In conclusion, the estimated flux distributions for the control lysine fermentation are consistent with the tracer studies documented in the literature and represent well the true state of the metabolism.

Table IV. Summary of f_{PPP} measurements reported in the literature.

f_{PPP} (%)	Organism	Tracer[a]	Reference
26[b]	*B. ammoniagenes*	Radio	40
38[c]	*B. ammoniagenes*	Radio	40
18[d]	*B. ammoniagenes*	Radio	39
36[e]	*B. ammoniagenes*	Radio	39
11[f]	*B. flavum*	Radio	58
16–21[f]	*B. flavum* and *C. glutamicum*	Radio	41
13[g]	*Microbacterium ammoniaphilum*	Stable	85
44[h]	*C. glutamicum*	Stable	22
44[i]	*C. glutamicum*	Stable	87

[a] Glucose labeled with stable or radio isotope.
[b] Stationary cells producing glutamate; low biotin.
[c] Stationary cells producing glutamate; high biotin.
[d] As above (footnote b) but without ammonium.
[e] As above (footnote c) but without ammonium.
[f] Washed cells plus arsenite; glutamate producer.
[g] Growing cells producing glutamate.
[h] Growing cells producing histidine.
[i] Growing cells producing lysine.

ATP Supply and Demand

Reaction 34 denotes the amount of ATP that is synthesized over that which is consumed in all other reactions and as such it represents ATP utilized for maintenance, futile cycles, etc. However, it must be interpreted with caution. During rapid growth, one might expect that futile cycle activity would be low and that all ATP generated would contribute toward maintenance requirements. On the contrary, when the culture enters the stationary phase due to threonine limitation, actual ATP requirements should be low and futile cycles activity high to expend excess energy produced by the clearly active primary metabolism. A large flux through reaction 34 does not, therefore, always equate to high maintenance requirements; true maintenance requirements are probably best estimated during rapid growth or product synthesis periods when operation of futile cycles are expected to be low. Consequently, the ATP flux depicted in Figure 5 (approximately 530 normalized units) should better reflect true maintenance requirements due to the high biomass and lysine synthesis rates associated with this period. From an analysis of theoretical flux distributions,[68] a lysine yield of approximately 65% could be supported while generating sufficient ATP to satisfy maintenance requirements (530 units) under a zero growth condition. This conclusion is also corroborated by chemostat studies.[28] Consequently, both analyses indicate that lysine yield in the stationary phase is not ATP limited. Indeed, lysine yields as high as 55% have been reported on complex media.[62] If not energy limited, the low observed lysine yields in Phases II

and III must result from suboptimal partitioning of carbon at the principal nodes.

Principal Node Analysis

Principal node analysis[68] involves the monitoring of principal node split-ratios (defined as the carbon flux channeled through a branch normalized by the total flux into the node) under various conditions. If the split-ratio of a particular principal node remains unchanged during a perturbation, then the node is potentially rigid. Similarly, if a node split-ratio significantly alters under perturbations, the node is potentially flexible. Analysis of the principal nodes during the first three phases of the fermentation, from the flux distributions illustrated in Figures 4 to 7, does provide some indication of their flexibility. However, because metabolite effector concentrations strongly govern nodal rigidity, the information provided from global perturbations induced by shifts in biomass synthesis rates must be interpreted with caution, and more local perturbations are needed to elucidate local aspects of nodal rigidity. Split-ratio variation for the Glc6P, PEP, Pyr, and OaA nodes are examined below.

Split-ratios at the Glc6P principal node are directly given in Figures 4 to 7 because they are already normalized with respect to the trunk (i.e., feed) flux, reaction 1. As discussed previously, the transition from phase I to phase II conditions results in a dramatic increase in the PPP split-ratio at the Glc6P node. The 69% PPP split-ratio (Fig. 5), as well as the specific amount of NADPH generated (1.38 mol/mol glucose), could support a lysine yield of 53% if biomass synthesis were zero. This preliminary analysis indicates that the Glc6P node is potentially flexible, implying that NADPH availability does not limit lysine yield. Further evidence in support of this conclusion will be presented in subsequent publications.

The OaA-branch split-ratio at the PEP principal node (Fig. 8) also exhibits a similar increase during the transition from growth to lysine production (Fig. 8B). At first inspection, this increase appears small compared with the perturbation exhibited at the Glc6P node, but this is not the case because lysine yield is quite sensitive to the split-ratio at the PEP node. For instance, the OaA branch split-ratio of 28% could produce a lysine yield of 50% if CO_2 was the sole by-product, although it cannot be determined from this analysis whether the OaA-branch split-ratio would remain at a 28% split if more carbon reached this node, as would occur under a zero growth condition.

The lysine-branch split-ratio at the Pyr principal node (Fig. 9) shows a maximum of 31% at the start of lysine production (Fig. 9B). This maximum could support a theoretical lysine yield of only 31%; hence, flux partitioning at the Pyr node does not exceed that required to meet the observed lysine yield. This does not necessarily imply that the Pyr node is rigid because inadequate amounts of either NADPH or OaA, due suboptimal split-ratios at either the Glc6P or PEP nodes, would limit lysine yield

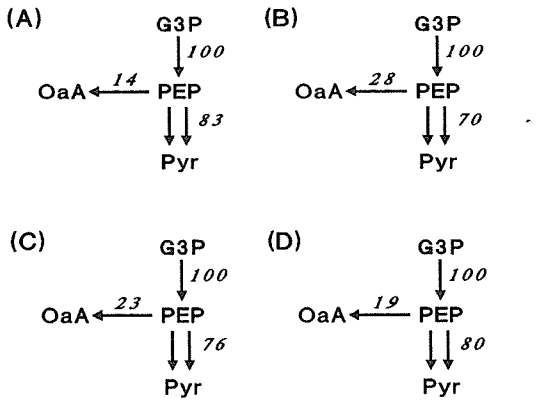

Figure 8. PEP principal node split-ratios for the lysine fermentation during (A) phase I (11.5 h), (B) early phase II (13.5 h), (C) late phase II (15.8 h), and (D) phase III (19.8 h). Double arrows indicate summation of PK and PTS fluxes.

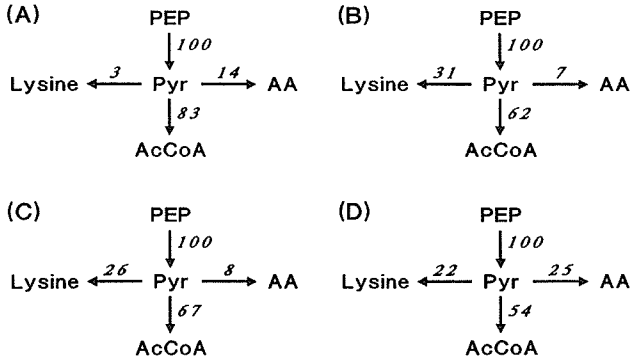

Figure 9. Pyruvate principal node split-ratios for the lysine fermentation during (A) phase I (11.5 h), (B) early phase II (13.5 h), (C) late phase II (15.8 h), and (D) phase III (19.8 h). Synthesis of alanine, valine, and lactate are lumped into the AA branch flux.

and the observed flux at the Pyr node.[68] Furthermore, during phase III of the fermentation, the TCA branch split-ratio decreases and the split-ratio for other amino acids (AA) increase. This implies that the TCA cycle may not outcompete dihydrodipicolinate synthase (lumped in reaction 31) for pyruvate, although the synthesis of Val, Ala, etc., might.

The split-ratios between the aspartate (Asp) and glutamate (Glut) branches at the OaA node are illustrated in Figure 10. It should be noted that malate dehydrogenase, reaction 16, is not considered a trunk flux of the OaA node, since this flow cannot be diverted from the TCA cycle due to mass balance constraints; that is, reaction 16 represents the actual amount of flux supported by the TCA cycle which passes through OaA. The difference between reactions 11 and 16 represent the net flux to Glut. Although under pure growth conditions the split between Asp and Glut synthesis is equal (Fig. 10A), it is quite apparent that when lysine synthesis begins the majority of OaA synthesized from PEP leads to Asp formation. Consequently, it is obvious why the OaA node is not considered a principal node for lysine fermentation.[68]

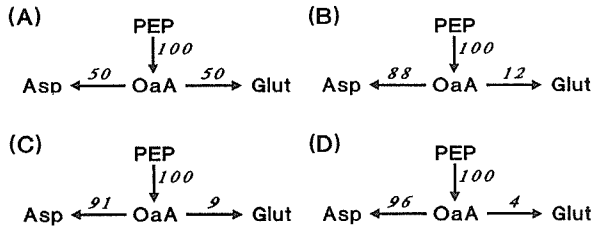

Figure 10. Oxaloacetate node split-ratios for the lysine fermentation during (A) phase I (11.5 h), (B) early phase II (13.5 h), (C) late phase II (15.8 h), and (D) phase III (19.8 h). Reaction 9, PEP carboxylase, is the only true feed of the OaA node.

SUMMARY

Analysis of the *C. glutamicum* metabolic network, constructed from literature data, identified several dependent reactions (singular groups) associated with anaplerotic reactions believed to be expressed in glutamic acid bacteria. Guided by these findings, intracellular assays were conducted in an attempt to identify the dominant pathways and thereby alleviate the singularity problems. Contrary to publications on *B. flavum,* the glyoxylate bypass appears repressed in the presence of glucose leaving PPC as the sole anaplerotic pathway expressed in *C. glutamicum* ATCC 21253. Flux distributions in the *C. glutamicum* metabolic network, constructed from fermentation data, indicate that the PPP and PPC support substantial flux during growth and lysine overproduction, a result consistent with tracer studies. From flux data during the transition from growth to lysine overproduction, it appears that the Glc6P branch point may be flexible, but the data are insufficient to draw any conclusions regarding the PEP or Pyr principal nodes.

Theoretical flux analysis is quite useful for the consolidation and validation of metabolic networks, identification of key branch points, and determination of maximum theoretical yields. However, there are limitations as to the extent of results that can be obtained from experimental flux distributions constructed from unperturbed systems. In subsequent publications it will be demonstrated that flux analysis during experimentally induced local metabolic perturbations can be used to further elucidate and clarify possible sources of metabolic rigidity. In the case of lysine overproduction by *C. glutamicum,* perturbation studies indicate that the Glc6P and Pyr nodes are flexible, and lysine yield appears constrained by the flexibility of the PEP node.[68,79]

We acknowledge the contribution of Professor A. J. Sinskey and Dr. M. Follettie of the MIT Department of Biology in our work on the analysis of *C. glutamicum* metabolism. Financial assistance was provided by the National Science Foundation, in part through PYI grant (No. CBT-8514729) and in part through the MIT Biotechnology Process Engineering Center. Lysine fermentations were conducted in equipment donated by Sulzer Biotech Systems.

The DOS-based computer program, *BIONET,* written for the construction, singularity analysis, consistency analysis, and calculation of flux distributions in metabolic networks can be obtained free of charge by contacting the corresponding author.

APPENDIX

This Appendix contains the biochemical reactions and metabolites that were used to construct the metabolic network of *Corynebacterium glutamicum* ATCC 21253, and a brief example illustrating the effect of singular groups on flux estimation.

C. glutamicum Biochemistry

Reaction numbers correspond to those reference in the main text and represent the elements of $\mathbf{x}(t)$ in Eq. (2).

PEP: glucose phosphotransferase system
(1) GLC + PEP = GLC6P + PYR

Storage compound; trehalose
(2) GLC6P + 0.5 ATP = 0.5 TREHAL + 0.5 ADP

Embden–Meyerhof–Parnas pathway
(3) GLC6P = FRU6P
(4) FRU6P + ATP = 2 GAP + ADP
(5) GAP + ADP + NAD = NADH + G3P + ATP
(6) G3P = PEP + H_2O
(7) PEP + ADP = ATP + PYR
(8) PYR + NADH = LAC + NAD

Anaplerotic reaction; PEP carboxylase
(9) PEP + CO_2 = OAA

Tricarboxylic acid cycle
(10) PYR + COA + NAD = ACCOA + CO_2 + NADH
(11) ACCOA + OAA + H_2O = ISOCIT + COA
(12) ISOCIT + NADP = AKG + NADPH + CO_2
(13) AKG + COA + NAD = SUCCOA + CO_2 + NADH
(14) SUCCOA + ADP = SUC + COA + ATP
(15) SUC + H_2O + FAD = MAL + FADH
(16) MAL + NAD = OAA + NADH

Acetate production or consumption
(17) ACCOA + ADP = AC + COA + ATP

Glutamate, glutamine, alanine, and valine production
(18) NH3 + AKG + NADPH = GLUT + H_2O + NADP
(19) GLUT + NH_3 + ATP = GLUM + ADP
(20) PYR + GLUT = ALA + AKG
(21) 2 PYR + NADPH + GLUT = VAL + CO_2 + H_2O +NADP + AKG

Pentose phosphate pathway
(22) GLC6P + H_2O + 2 NADP = RIBU5P + CO_2 +2 NADPH
(23) RIBU5P = RIB5P
(24) RIBU5P = XYL5P
(25) XYL5P + RIB5P = SED7P + GAP
(26) SED7P + GAP = FRU6P + E4P
(27) XYL5P + E4P = FRU6P + GAP

Oxidative phosphorylation; P/O = 2
(28) 2 NADH + O_2 + 4 ADP = 2 H_2O + 4 ATP + 2 NAD
(29) 2 FADH + O_2 + 2 ADP = 2 H_2O + 2 ATP + 2 FAD

Aspartate amino acid family
(30) OAA + GLUT = ASP + AKG
(31) ASP + PYR + 2 NADPH + SUCCOA + GLUT + ATP = SUC + AKG + CO_2 + LYSI + 2 NADP +COA + ADP
(32) LYSI = LYSE

Biomass synthesis; $C_{3.97}$, $H_{6.46}$, $O_{1.94}$, $N_{0.845}$, and 3.02% ash
(33) 0.021 GLC6P + 0.007 FRU6P + 0.09 RIB5P + 0.036 E4P +0.013 GAP + 0.15 G3P + 0.052 PEP + 0.03 PYR +0.332 ACCOA + 0.08 ASP + 0.033 LYSI + 0.446 GLUT +0.025 GLUM + 0.054 ALA + 0.04 VAL + 0.052 THR +0.015 MET + 0.043 LEU + 3.82 ATP + 0.476 NADPH +0.312 NAD = BIOMAS + 3.82 ADP + 0.364 AKG +0.476 NADP + 0.312 NADH + 0.143 CO_2

ATP dissipation reaction

(34) ATP = ADP

Metabolite Accumulation Rate Vector

Mass balances were constructed around the following metabolites and represent the element of $\mathbf{r}(t)$ in Eq. (2).

(1) AC	Acetate
(2) ACCOA	Acetyl coenzyme A
(3) AKG	α-Ketoglutarate
(4) ALA	Alanine
(5) ASP	Aspartate
(6) ATP	Adenosine 5′-triphosphate
(7) BIOMAS	Biomass
(8) CO_2	Carbon dioxide
(9) E4P	Erythrose-4-phosphate
(10) FADH	Flavin adenine dinucleotide, reduced
(11) FRU6P	Fructose-6-phosphate
(12) G3P	3-Phosphoglycerate
(13) GAP	Glyceraldehyde-3-phosphate
(14) GLC	Glucose
(15) GLC6P	Glucose-6-phosphate
(16) GLUM	Glutamine
(17) GLUT	Glutamate
(18) ISOCIT	Isocitrate
(19) LAC	Lactate
(20) LYSE	Lysine, extracellular
(21) LYSI	Lysine, intracellular
(22) MAL	Malate
(23) NADH	Nicotinamide adenine dinucleotide, reduced
(24) NADPH	Nicotinamide adenine dinucleotide phosphate, reduced
(25) NH_3	Ammonia
(26) O_2	Oxygen
(27) OAA	Oxaloacetate
(28) PEP	Phosphoenolpyruvate
(29) PYR	Pyruvate
(30) RIB5P	Ribose-5-phosphate
(31) RIBU5P	Ribulose-5-phosphate
(32) SED7P	Sedoheptulose-7-phosphate
(33) SUC	Succinate
(34) SUCCOA	Succinate coenzyme A
(35) TREHAL	Trehalose
(36) VAL	Valine
(37) XYL5P	Xylulose-5-phosphate

Singular Groups

If the lumped reaction for the glyoxylate shunt, given by

(35) ISOCIT + ACCOA + H2O = SUC + MAL + COA,

is added as reaction 35 to the metabolic network given above, the stoichiometry matrix, **A**, of Eq. (2) becomes singular. Since **A** is only one dimension short of full rank, only one additional measurement needs to be specified. However, examination of the vector that spans the one-dimensional null space of **A** reveals that the singular group consists of reactions 3, 4, 5, 6, 7, 9, 10, 11, 12, 13, 14, 15, 16, 22, 23, 24, 25, 26, 27, 28, 29, 34, and 35. Any additional measurement which specifies the flux of any of the reactions listed in the singular group will suffice to remove the singularity; however, all reactions in the singular group will be affected by the value of the specified flux. This explains why the flux distributions illustrated in Figure 1A and B are radically different from one another and the importance of properly constraining an extended singular group. As an example of a more local singular group, the addition of the lumped reaction for the alternate lysine synthesis pathway, given by

(36) ASP + PYR + 3 NADPH + ATP + NH3 = LYSI
+ CO2 + 3 NADP + ADP + 2 H2O,

results in a singular group that consists only of reactions 14, 18, 31, 34, and 35. Consequently, lumping this reaction together with reaction 31 (i.e., setting the flux of reaction 35 to zero) only affects reactions 14, 18, and 34 in the network.

References

1. Aris, R., Mah, R. H. S. 1963. Independence of chemical reactions. I&EC Fund. **2**: 90–94.
2. Atkinson, D. E. 1977. Cellular energy metabolism and its regulation. Academic Press, New York, pp. 116–118.
3. Bailey, J. E. 1991. Toward a science of metabolic engineering. Science **252**: 1668–1675.
4. Baryshnikova, L. M., Loginova, N. V. 1979. Carboxylases of coryneform bacteria. Microbiol. **48**: 787–789.
5. Bergmeyer, H. U., Beutler, H.-O. 1983. Ammonia. pp. 454–461. In: H. U. Bergmeyer (ed.), Methods of enzymatic analysis. 3rd edition, vol. 8. Verlag Chemie, Weinheim.
6. Blumm, J. J., Stein, R. B. 1982. On the analysis of metabolic networks, pp. 99–125. In: R. F. Goldberger and K. R. Yamamoto (eds.), Biological regulation and development, vol. 3A. Plenum Press, New York.
7. Brown, D. E., Gaddum, R. N. 1988. Linear growth in batch culture caused by conservative trace nutrient limitations. Biotechnol. Lett. **10**: 525–530.
8. Cabib, E., Leloir, L. F. 1958. The biosynthesis of trehalose phosphate. J. Biol. Chem. **231**: 259–275.
9. Cooper, R. A., Kornberg, H. L. 1969. Phosphoenolpyruvate synthetase. Meth. Enzymol. **13**: 309–314.
10. Coppella, S. J., Dhurjati, P. 1987. Low-cost computer-coupled fermentor off-gas analysis via quadrupole mass spectrometer. Biotechnol. Bioeng. **29**: 679–689.
11. Cremer, J., Eggeling, L., Sahm, H. 1991. Control of the lysine biosynthesis sequence in *Corynebacterium glutamicum* as analyzed by overexpression of the individual corresponding genes. Appl. Environ. Microbiol. **57**: 1746–1752.
12. Cremer, J., Treptow, C., Eggeling, L., Sahm, H. 1988. Regulation of enzymes of lysine biosynthesis in *Corynebacterium glutamicum.* J. Gen. Microbiol. **134**: 3221–3229.
13. Crueger, W., Crueger, A. 1984. Strain development, pp. 9–48. In: T. D. Brock (ed.), Biotechnology: A textbook of industrial microbiology. Sinauer Associates, Sunderland, MA.
14. Darton, H. H., Gunsalus, I. C. 1969. Citratase and isocitratase. Meth. Enzymol. **5**: 622–633.
15. Delgado, J. P., Liao, J. C. 1991. Identifying rate-controlling enzymes in metabolic pathways without kinetic parameters. Biotechnol. Prog. **7**: 15–20.
16. Goldberg, D. M., Ellis, G. 1983. Isocitrate dehydrogenase, pp. 183–190. In: H. U. Bergmeyer (ed.), Methods of enzymatic analysis. 3rd edition, vol. 3. Verlag Chemie, Weinheim.
17. Gottschalk, G. 1986. Bacterial metabolism. 2nd edition. Springer-Verlag, New York, pp. 40–42.
18. Hoischen, C., Kramer, R. 1989. Evidence for an efflux carrier system involved in the secretion of glutamate by *Corynebacterium glutamicum.* Arch. Microbiol. **151**: 342–347.
19. Holms, W. H. 1986. The central metabolic pathways of *Escherichia coli:* Relationship between flux and control at a branch point, efficiency of conversion to biomass, and excretion of acetate. Curr. Topics Cell. Reg. **28**: 69–105.
20. Hsu, R. Y., Lardy, H. A. 1969. Malic enzyme. Meth. Enzymol. **13**: 230–235.
21. Inbar, L., Lapidot, A. 1987. ^{13}C-NMR, ^{1}H-NMR and gas-chromatography mass-spectrometry studies of the biosynthesis of ^{13}C-enriched L-lysine by *Brevibacterium flavum.* Eur. J. Biochem. **162**: 621–633.
22. Ishino, S., Kuga, T., Yamaguchi, K., Shirahata, K., Araki, K. 1986. ^{13}C NMR studies of histidine fermentation with a *Corynebacterium glutamicum* mutant. Agric. Biol. Chem. **50**: 307–310.

23. Jeong, J. W., Snay, J., Ataai, M. M. 1990. A mathematical model for examining growth and sporulation processes of *Bacillus subtilis.* Biotechnol. Bioeng. **35**: 160–184.
24. Kawahara, Y., Tanaka, T., Ikeda, S., Sone, N. 1988. Coupling sites of the respiratory chain of *Brevibacterium lactofermentum.* Agric. Biol. Chem. **52**: 1979–1983.
25. Kinoshita, S. 1985. Glutamic acid bacteria, pp. 115–142. In: A. L. Demain and N. A. Solomon (eds.), Biology of industrial microorganisms. Benjamin/Cummings, London.
26. Kinoshita, S., Tanaka, K. 1972. Glutamic acid, pp. 263–324. In: K. Yamada (ed.), The microbial production of amino acids. Wiley, New York.
27. Kiss, R. D., Stephanopoulos, G. 1991. Metabolic activity control of the L-lysine fermentation by restrained growth fed-batch strategies. Biotechnol. Prog. **7**: 501–509.
28. Kiss, R. D., Stephanopoulos, G. 1992. Metabolic characterization of a L-lysine producing strain by continuous culture. Biotechnol. Bioeng. **39**: 565–574.
29. Kornberg, H. L. 1966. Anaplerotic sequences and their role in metabolism. Essays Biochem. **2**: 1–31.
30. Lawson, C. L., Hanson, R. J. 1974. Solving least squares problems. Prentice-Hall, Engelwood Cliffs, NJ.
31. Mandelstam, J., McQuillen, K., Dawes, I. 1982. Biochemistry of bacterial growth. 3rd edition. Halsted Press, New York, p. 172.
32. Menkel, E., Theirbach, G., Eggeling, L., Sahm, H. 1989. Influence of increased aspartate availability on lysine formation by a recombinant strain of *Corynebacterium glutamicum* and utilization of fumarate. Appl. Microbiol. Biotechnol. **55**: 684–688.
33. Misono, H., Ogasawara, M., Nagasaki, S. 1986. Characterization of *meso*-diaminopimelate dehydrogenase from *Corynebacterium glutamicum* and its distribution in bacteria. Agric. Biol. Chem. **50**: 2729–2734.
34. Mori, M., Shiio, I. 1987. Pyruvate formation and sugar metabolism in an amino acid-producing bacterium, *Brevibacterium flavum.* Agric. Biol. Chem. **51**: 129–138.
35. Nakatani, Y., Fujioka, M., Higashino, K. 1972. Enzymatic determination of L-lysine in biological materials. Anal. Biochem. **49**: 225–231.
36. Niranjan, S. C., San, K.-Y. 1989. Analysis of a framework using material balances in metabolic pathways to elucidate cellular metabolism. Biotechnol. Bioeng. **34**: 496–501.
37. Noltman, E. A. 1977. Phosphoglucose isomerase. Meth. Enzymol. **9**: 557–575.
38. Noorman, H. J., Heijnen, J. J., Luyben, K. Ch. A. M. 1991. Linear relations in microbial reaction systems: A general overview of their origin, form, and use. Biotechnol. Bioeng. **38**: 603–618.
39. Oishi, K., Aida, H. 1964. Studies on amino acid fermentation. Part XII. Effect of NH_4 on the catabolism of glucose by a glutamic acid-producting bacterium, *Brevibacterium ammoniagenes* 317-1. Amino Acid Nucleic Acid **10**: 6–11.
40. Oishi, K., Aida, H. 1965. Studies on amino acid fermentation. Part XI. Effect of biotin on the Embden–Meyerhof–Parnas pathway and the hexose–monophosphate shunt in a glutamic acid-producing bacterium, *Brevibacterium ammoniagenes* 317-1. Agric. Biol. Chem. **29**: 83–89.
41. Otsuka, S.-I., Miyajima, R., Shiio, I. 1965. Comparitive studies on the mechanism of microbial glutamate formation. I. Pathways of glutamate formation from glucose in *Brevibacterium flavum* and in *Micrococcus glutamicus.* J. Gen. Appl. Microbiol. **11**: 285–294.
42. Otsuka, S.-I., Miyajima, R., Shiio, I. 1965. Comparative studies on the mechanism of microbiol glutamate formation. II. Effect of biotin. J. Gen. Appl. Microbiol. **11**: 295–301.
43. Ozaki, H., Shiio, I. 1968. Regulation of the TCA and glyoxylate cycles in *Brevibacterium flavum.* I. Inhibition of isocitrate lyase and isocitrate dehydrogenase by organic acids related to the TCA and glyoxylate cycles. J. Biochem. **64**: 355–363.
44. Ozaki, H., Shiio, I. 1983. Production of lysine by pyruvate kinase mutants of *Brevibacterium flavum.* Agric. Biol. Chem. **47**: 1569–1576.
45. Palsson, B. O., Lightfoot, E. N. 1985. Mathematical modeling of dynamics and control in metabolic networks. V. Static bifurcations in single biochemical control loops. J. Theor. Biol. **113**: 279–298.
46. Papoutsakis, E. T. 1984. Equations and calculations for fermentations of butyric acid bacteria. Biotechnol. Bioeng. **26**: 174–187.
47. Reed, L. J., Willms, C. R. 1966. Purification and resolution of the pyruvate dehydrogenase complex (*Escherichia coli*). Meth. Enzymol. **9**: 247–265.
48. Rodwell, V. W. 1969. Biosynthesis of amino acids and related compounds, pp. 334–351. In: D. M. Greenberg (ed.), Metabolic pathways. 3rd edition, vol. 3. Academic Press, New York.
49. Ruklish, M. P., Marauska, D. F., Viestur, U. E. 1978. Nature of the regulation of enzymes of glucose and acetic acid metabolism in lysine-forming *Brevibacterium flavum.* Microbiol. **47**: 804–808.
50. Sano, K., Ito, K., Miwa, K., Nakamori, S. 1987. Amplification of the phosphoenol pyruvate carboxylase gene of *Brevibacterium lactofermentum* to improve amino acid production. Agric. Biol. Chem. **51**: 597–599.
51. Schrumpf, B., Schwarzer, A., Kalinowski, J., Puhler, A., Eggeling, L., Sahm, H. 1991. A functionally split pathway for lysine synthesis in *Corynebacterium glutamicum.* J. Bacteriol. **173**: 4510–4516.
52. Shiio, I., Momose, H., Oyama, A. 1992. Genetic and biochemical studies on bacterial formation of L-glutamate. I. Relationship between isocitrate lyase, acetate kinase, and phosphate acetyltransferase levels and glutamate production in *Brevibacterium flavum.* J. Gen. Appl. Microbiol. **15**: 27–40.
53. Shiio, I., Mori, M., Ozaki, H. 1982. Amino acid aminotransferases in an amino acid-producing bacterium, *Brevibacterium flavum.* Agric. Biol. Chem. **46**: 2967–2977.
54. Shiio, I., Otsuka, S.-I., Katsuya, N. 1962. Effect of biotin on the bacterial formation of glutamic acid. II. Metabolism of glucose. J. Biochem. **52**: 108–116.
55. Shiio, I., Otsuka, S.-I., Takahashi, M. 1961. Significance of α-ketoglutaric dehydrogenase on the glutamic acid formation in *Brevibacterium flavum.* J. Biochem. **50**: 164–165.
56. Shiio, I., Otsuka, S.-I., Tsunoda, T. 1959. Glutamic acid formation from glucose by bacteria. I. Enzymes of the Embden–Meyerhof–Parnas pathway, the Krebs cycle, and the glyoxylate bypass in cell extracts of *Brevibacterium flavum.* J. Biochem. **46**: 1303–1311.
57. Shiio, I., Otsuka, S.-I., Tsunoda, T. 1960. Glutamic acid formation from glucose by bacteria. IV. Carbon dioxide fixation and glutamate formation in *Brevibacterium flavum* No. 2247. J. Biochem. **48**: 110–120.
58. Shiio, I., Otsuka, S.-I., Tsunoda, T. 1960. Glutamic acid formation from glucose by bacteria. III. On the pathway of pyruvate formation in *Brevibacterium flavum* No. 2247. J. Biochem. **47**: 414–421.
59. Shiio, I., Ozaki, H., Ujigawa-Takeda, K. 1982. Production of aspartic acid and lysine by citrate synthase mutants of *Brevibacterium flavum.* Agric. Biol. Chem. **46**: 101–107.
60. Shiio, I., Sugimoto, S.-I., Kawamura, K. 1990. Effects of carbon source sugars on the yield of amino acid production and sucrose metabolism in *Brevibacterium flavum.* Agric. Biol. Chem. **54**: 1513–1519.
61. Shiio, I., Sugimoto, S.-I., Toride, Y. 1984. Studies on mechanisms for lysine production by pyruvate kinase-deficient mutants of *Brevibacterium flavum.* Agric. Biol. Chem. **48**: 1551–1558.
62. Shiio, I., Toride, Y., Sugimoto, S.-I. 1984. Production of lysine by pyruvate dehydrogenase mutants of *Brevibacterium flavum.* Agric. Biol. Chem. **48**: 3091–3098.
63. Shiio, I., Ujigawa, K. 1978. Enzymes of the glutamate and aspartate synthetic pathways in a glutamate-producing bacterium, *Brevibacterium flavum.* J. Biochem. **84**: 647–657.
64. Shiio, I., Ujigawa-Takeda, K. 1980. Presence and regulation of α-ketoglutarate dehydrogenase complex in a glutamate-producing bacterium, *Brevibacterium flavum.* Agric. Biol. Chem. **44**: 1897–1904.

65. Shiio, I., Yokota, A., Sugimoto, S.-I. 1987. Effect of pyruvate kinase deficiency on L-lysine productivities of mutants with feedback-resistant aspartokinases. Agric. Biol. Chem. **51**: 2485–2493.
66. Shvinka, Yu. E., Viestur, U. E., Toma, M. K. 1979. Alternative pathways of oxidation in the respiratory chain of *Brevibacterium flavum.* Microbiol. **48**: 4–10.
67. Sorribas, A., Savageau, M. 1989. A comparison of variant theories of intact biochemical systems. II. Flux-oriented and metabolic control theories. Math. Biosci. **94**: 195–238.
68. Stephanopoulos, G., Vallino, J. J. 1991. Network rigidity and metabolic engineering in metabolite overproduction. Science **252**: 1675–1681.
69. Sugimoto, S.-I., Shiio, I. 1989. Regulation of enzymes for erythrose 4-phosphate synthesis in *Brevibacterium flavum.* Agric. Biol. Chem. **53**: 2081–2087.
70. Sugimoto, S.-I., Shiio, I. 1989. Fructose metabolism and regulation of 1-phosphofructokinase and 6-phosphofructokinase in *Brevibacterium flavum*. Agric. Biol. Chem. **53**: 1261–1268.
71. Toennies, G. 1965. Role of amino acids in postexponential growth. J. Bacteriol. **90**: 438–442.
72. Tosaka, O, Hirakawa, H., Yoshihara, Y., Takinami, K., Hirose, Y. 1978. Production of L-lysine by alanine auxotrophs derived from AEC resistant mutants of *Brevibacterium flavum.* Agric. Biol. Chem. **42**: 1773–1778.
73. Tosaka, O, Morioka, H., Takinami, K. 1979. The role of biotin dependent pyruvate carboxylase in L-lysine production. Agric. Biol. Chem. **43**: 1513–1519.
74. Tosaka, O, Takinami, K., Hirose, Y. 1978. L-Lysine production by *S*-(2-aminoethyl) L-cysteine and α-amino-β-hydroxyvaleric acid resistant mutants of *Brevibacterium lactofermentum.* Agric. Biol. Chem. **42**: 745–752.
75. Tosaka, O., Yoshihara, Y., Ikeda, S., Takinami, K. 1985. Production of L-lysine by fluoropyruvate-sensitive mutants of *Brevibacterium flavum.* Agric. Biol. Chem. **49**: 1305–1312.
76. Tsai, S. P., Lee, Y. H. 1988. Application of metabolic pathway stoichiometry to statistical analysis of bioreactor measurement data. Biotechnol. Bioeng. **32**: 713–715.
77. Tsai, S. P., Lee, Y. H. 1988. Application of Gibb's rule and a simple pathway method to microbial stoichiometry. Biotechnol. Prog. **4**: 82–88.
78. Tsuchida, T., Momose, H. 1975. Genetic changes of regulatory mechanisms occurred in leucine and valine producing mutants derived from *Brevibacterium lactofermentum* 2256. Agric. Biol. Chem. **39**: 2193–2198.
79. Vallino, J. J. 1991. Identification of branch-point restrictions in microbial metabolism through metabolic flux analysis and local network perturbations, Ph.D. thesis, Massachusetts Institute of Technology, Cambridge, MA.
80. Vallino, J. J., Stephanopoulos, G. 1987. Intelligent sensors in biotechnology: applications for the monitoring of fermentations and cellular metabolism. Ann. NY Acad. Sci. **506**: 415–430.
81. Vallino, J. J., Stephanopoulos, G. 1990. Flux determination in cellular bioreaction networks: applications to lysine fermentations, pp. 205–219. In: S. K. Sikdar, M. Bier, and P. Todd. (eds.), Frontiers in bioprocessing. CRC Press, Boca Raton, FL.
82. Vandecasteele, J. P., Lemal, J., Coudert, M. 1975. Pathways and regulation of glutamate synthesis in a *Corynebacterium* sp. overproducing glutamate. J. Gen. Microbiol. **90**: 178–180.
83. Verhoff, F. H., Spradlin, J. E. 1976. Mass and energy balance analysis of metabolic pathways applied to citric acid production by *Aspergillus niger.* Biotechnol. Bioeng. **18**: 425–432.
84. von der Osten, C. H., Gioannetti, C., Sinskey, A. J. 1989. Design of a defined medium for growth of *Corynebacterium glutamicum* in which citrate facilitates iron uptake. Biotechnol. Lett. **11**: 11–16.
85. Walker, T. E., Han, C. H., Kollman, V. H., London, R. E., Matwiyoff, N. A. 1982. ^{13}C Nuclear magnetic resonance studies of the biosynthesis by *Microbacterium ammoniaphilum* of L-glutamate selectively enriched with carbon-13. J. Biol. Chem. **257**: 1189–1195.
86. Wang, N. S., Stephanopoulos, G. 1983. Application of macroscopic balances to the identification of gross measurement errors. Biotechnol. Bioeng. **25**: 2177–2208.
87. Yamaguchi, K., Ishino, S., Araki, K., Shirahata, K. 1986. ^{13}C NMR studies of lysine fermentation with a *Corynebacterium glutamicum* mutant. Agric. Biol. Chem. **50**: 2453–2459.
88. Yokota, A., Shiio, I. 1988. Effects of reduced citrate synthase activity and feedback-resistant phosphoenolpyruvate carboxylase on lysine productivities of *Brevibacterium flavum.* Agric. Biol. Chem. **52**: 455–463.